TRIBHUVAN UNIVERSITY

INSTITUTE OF ENGINEERING

PULCHOWK CAMPUS

THESIS NO.: 076MSMSE007

Development and Characterization of Bacteria based Self-healing Concrete

by

Gaurab Raj Neupane

A THESIS

SUBMITTED TO THE DEPARTMENT OF APPLIED SCIENCES AND CHEMICAL ENGINEERING IN PARTIAL FULFILLMENT OF THE REQUIREMENTS FOR THE DEGREE OF MASTER OF SCIENCE IN MATERIAL SCIENCE AND ENGINEERING

DEPARTMENT OF APPLIED SCIENCES AND CHEMICAL ENGINEERING

LALITPUR, NEPAL

APRIL, 2023

COPYRIGHT

ACKNOWLEDGEMENT

It is to express sincere thanks and gratitude to supervisor, Prof. Dr. Gokarna Bahadur Motra and Prof. Dr. Hem Raj Panta for incessant guidance, comments, suggestions, and motivation. This is the opportunity to thank the Department of Applied Science and Chemical Engineering, and Department of Civil Engineering, Pulchowk Campus and all the faculty members for their help during this project. Thanks, are must to Laxmi Prasad Thapa, MD, Himalaya Research Institute of Biotechnology for providing the bacteria required.

Sincere thanks and gratitude are due to Shivam Cements Pvt. Ltd. and Acme international Pvt. Ltd. for providing us with cement and high range water reducing admixture respectively without which the research work would not be possible.

Furthermore, acknowledgements are due to Mr. Amrit Acharya and Ms. Manita KC, Public Health Laboratory, Department of Civil Engineering, Pulchowk Campus for their support and motivation. We would also like to thank Mr. Keshab Bhattarai, Heavy Lab, Department of Civil Engineering and Mr. Tek Giri, Central Material Testing Laboratory, Department of Civil Engineering for their support with experimental tasks. Acknowledgements are a must to the Department of Pharmacy, Kathmandu University for providing the FTIR spectroscopy results.

Last but not the least, I would like to thank my family and colleagues, most notably Er. Adarsha Chauhan and Er. Anish Bhusal for their valuable time, resources and support.

Er. Gaurab Raj Neupane

076MSMSE007

ABSTRACT

It is highly typical for concrete structures to develop cracks as a result of different load and non-load causes, which shortens their useful lifespan. Hence, maintenance and repair procedures are required to stop cracks from spreading and shortening the service life of the buildings. However, access to the damaged areas may be challenging because of the high labour and material costs connected with the fixing and upkeeping of concrete structures. One potential approach is autonomous healing using bacteria-based self-healing agents in capsules. The bacteria are activated by water and oxygen availability when released from a broken capsule during this process. Aerobic digestion of bacteria produces calcite which in turn is used to fill up the microcracks in concrete.

This study concentrated on the experimental investigation of the self-healing property of concrete with encapsulated bacteria, *Bacillus Subtilis*. Calcium alginate was used as encapsulation material. Various tests were conducted for testing the beads produced. Compressive strength of concrete was found to be increased upon 2% concentration of calcium alginate beads (CAB) and bacteria encapsulated calcium alginate beads (BCAB). Further increment in concentration of beads resulted in decrement of compressive strength. Self-healing was achieved in certain concrete cracks but not in others.

Keywords: Concrete, Service Life, Self-healing, Bacteria, Water Permeability, Compressive Strength, SEM

TABLE OF CONTENTS

LIST OF TABLES

LIST OF FIGURES

LIST OF SYMBOLS

Φ	Diameter of the needle

LIST OF IMAGES

LIST OF ACRONYMS AND ABBREVIATIONS

MICP	Microbial Induced Calcite Precipitation
CSH	Calcium Silicate Hydrate
ATCC	American Type Culture Collection
CA	Coarse aggregate
FA	Fine aggregate
SSD	Saturated Surface Dry
ACI	American Concrete Institute
RCPT	Rapid Chloride Permeability Test
MPa	Megapascal
CAB	Calcium alginate bead
BCAB	Bacteria Infused Calcium Alginate Beads

CHAPTER 1: INTRODUCTION

1.1 Background

The Latin term "concretus" meaning compounded, is where the word "concrete" originates. It is a heterogeneous composite material made up of cement, coarse aggregate, fine aggregate, and water that was utilized by the ancient Romans to build walls and roofs.

Basically, two different types of concrete are used across the world: ordinary plain concrete and reinforced concrete. Ordinary plain concrete is formed by combining cement, fine aggregate, and coarse aggregate with water; when steel reinforcement is added to plain concrete, it is called reinforced concrete (Hassoun & Al-Manaseer, 2020). The most often utilized building material worldwide is concrete. It is the most affordable man-made construction material to make, is readily available worldwide, and is sturdy. Regrettably, concrete can sustain a wide range of damages that lead to fissures. These cracks may be roughly divided into two categories: I structural cracks, which result from design flaws, construction issues, and supervision issues; and (ii) non-structural cracks, which are brought on by environmental factors including temperature, humidity, and/or material quality. Freeze/thaw cycles, chemical assaults, corrosion, severe loads, and other environmental variables all result in deterioration to concrete under ambient circumstances. As a result, concrete structure maintenance is expensive and frequent. Several nations throughout the world spend countless billions of dollars annually on preserving their buildings and bridges. In Europe, rehabilitation and repair of existing structures are funded with 50% of the yearly construction budget. The mean cost of US bridge maintenance and repair is 5.3 billion dollars (van Tittelboom & de Belie, 2013). For the fiscal year of 2078/079, the budget of 12 Arba 50 crores was allocated for Strategic Road Network maintenance and rehabilitation and the budget of 24 crores 35 lakhs was allocated for local level roads maintenance in Nepal (SRN | Road Board Nepal, 2023).

The corrosion of reinforcement inside of concrete, which often results from an aggressive chemical assault, like when chloride penetrates concrete specifically through its fractures and dissolves the shielding layer around the reinforcement, has an important impact on the longevity of concrete. Loss of the bond between the concrete and the steel, as well as an increase in the size of the steel inside the concrete, are consequences of corrosion on the characteristics of concrete and lower the serviceability of concrete (Neville, 2011).

Hence, there have been several attempts to lessen the quantity and size of fractures that develop in concrete. For instance, using high-quality raw materials, having a proper mix design,

establishing suitable curing conditions, and having effective operation structure management. Concrete cracks, however, cannot be stopped from developing. Over past 25 years, researchers are working on self-healing concrete that would alleviate cost and improve utilitarian properties and service life of structures by recovering strength, water-tightness and porosity of the concrete. Autogenous and autonomous healing are the two basic processes that drive the process of self-healing.

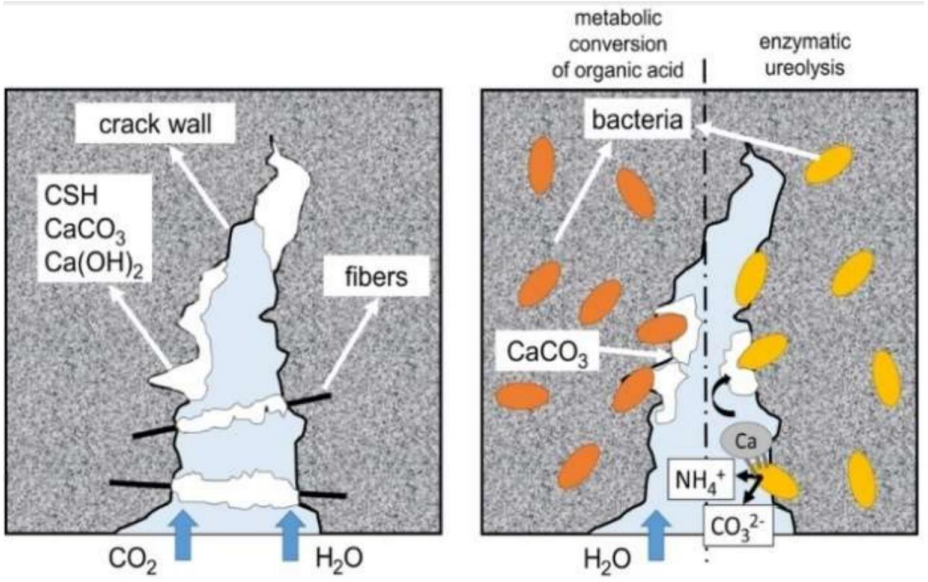

Figure 1: Left image represents metabolic conversion of organic acid and right image represents enzymatic ureolysis.

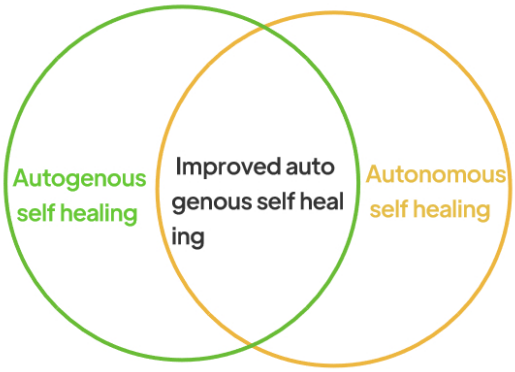

Figure 2: Self-healing types

Concrete may cure fractures up to a certain width owing to autogenous self-healing, which includes crystal precipitation. Crystals of calcium carbonate precipitate due to rection between carbon dioxide evolution owing to carbonation and calcium hydroxide (portlandite) present in concrete. Also, CSH crystals precipitate due to continual hydration of cement particles . This therapeutic method is significant in fresh concrete. (Mohammad et al., 2019).

In contrast, autonomous concrete healing promotes the use of extraneous elements such as bacteria and tiny containers containing healing chemicals to improve the concrete's capability for self-healing (Roy et al., 2020). Capsule-based self-healing (spherical or cylindrical) and vascular-based self-healing (active or passive) are two main methods that autonomic healing transports the healing substance.

There are two mechanisms in vascular based self-healing. Active mode is the first mode. This mode makes use of a vessel network that is linked to external glue supply for sharing purposes. The second form, known as the passive mode, does not have a connection to the external glue supply and instead distributes glue through capsules, hollow pipettes, and a network of vessels. Based on the two aforementioned techniques, self-healing concrete is produced using vessel networks and hollow pipettes. Researchers have developed a variety of self-healing materials, including polymers and polymeric materials, by using hollow pipettes with different length scales (Mohammad et al., 2019).

In these settings, the method of self-healing involves the production of calcium carbonate, whether by bacterial metabolism of an organic acid or the enzymatic ureolysis. Recent years have seen a lot of interest in bacteria-based self-healing concrete due to highly encouraging findings from small scale laboratory investigations (Roy et al., 2020).

Because they are compatible with concrete materials, calcareous deposition and other forms of concrete minerals can be useful and long-lasting. For instance, using concrete-compatible minerals to patch gaps enhances concrete's waterproofing while safeguarding the steel reinforcement beneath it from harmful substances like chlorides or other ions that hasten the corrosion process. Therefore, one of the primary goals of employing calcareous deposition to encourage bacteria is the recovery of utilitarian concrete qualities including water-tightness and mechanical strength. The convergence of calcium ions, pH solution concentration, concentration of dissolved inorganic carbon, and the presence of nucleation sites in the natural environment all have an impact on calcium carbonate precipitation (Hammes & Verstraete, 2002). The first three circumstances concern the concrete matrix but the last circumstance is dependent on the bacterial cell itself. Different heterotrophic bacterial assimilation and dissimulation routes that result in the generation of dissolved inorganic carbon might lead to bacterial precipitation. The three primary heterotrophic mechanisms that have received the most attention from researchers are bacterial metabolism's conversion of calcium lactate (anaerobic), urea hydrolysis, and nitrate reduction (aerobic). In the first method, crack holes

permit oxygen to enter the concrete and bacteria to convert calcium lactate to calcium carbonate and carbon dioxide along the broken surface (Roy et al., 2020). If there are portlandite crystals nearby, they could release carbon dioxide and produce additional calcium carbonate, which is also useful for healing. Urea breaking down to produce ammonium and carbonate ions resulting in precipitation of calcium carbonate is the second route (Van Tittelboom et al., 2010). Urease is an enzyme produced by *Bacillus Sphaericus* that acts as a catalyst. A negative bacterial cell attracts a calcium ion from a calcium source like calcium nitrate, which it then reacts with to precipitate calcium carbonate. Under low oxygen circumstances, the third route reduces nitrates to create carbonate and bicarbonate ions. (Erşan et al., 2016).

It has been demonstrated that bacteria put straight to concrete during the mixing process have little functioning over time. As a result, a variety of techniques have been developed to safeguard bacteria and bacteria-based agents (bacteria and mineral precursor chemicals) before they are applied to cementitious materials. Clay particle protection for bacteria-based agents (Wiktor & Jonkers, 2011) bacteria in diatomaceous earth and melamine-based microcapsules (J. Y. Wang et al., 2014) have increased the time period over which crack filling could be observed. However, these materials did not increase the capacity for healing of their respective systems. Alginate has recently been suggested as a protective container for bacterial spores (J. Wang et al., 2015) and as a component of a bacteria-based solution for potential uses in self-healing concrete. Alginate is a cheap biopolymer that swells into a hydrogel in the presence of water (Hoffman, 2012). It has been demonstrated that alginate hydrogels facilitate the synthesis of alginate-mineral biocomposites (Abramson et al., 2010; Alcântara et al., 2010; Olderay et al., 2009; Wu et al., 2014). The effectiveness of biological composites like nacre (mother-of-pearl) serves as a clear inspiration for the creation of biocomposites. The biocomposite material nacre, which contains more than 95% aragonite and 1% by volume polymer, possesses extraordinary strength, hardness, and toughness. It is twice as hard and 1,000 times tougher than aragonite polymer(Currey & Taylor, 1974; Wegst & Ashby, 2004). In order to create an organo-mineral biopolymer (or biocomposite) for filling concrete fractures, Bergdale et al. developed a bacterium (Bergdale et al., 2012).

Therefore, compared to other methods of self-healing, bacteria based self-healing were chosen for the thesis and calcium alginate was chosen as encapsulating material.

1.2 Rationale of the study

Some of the rationales of the study are as follows.

- The rationale of self-healing in the area of concrete materials is to improve its utilitarian properties and its service-life by recuperating strength
- and water-tightness of the concrete.
- Biomineralization by bacteria is used for filling microcracks in concrete.

1.3 Objective of the study

Some of the purposes of study are as follows.

- Investigate the effects of encapsulated bacteria in autonomous self-healing of concrete.
- Investigate the effects of Calcium alginate beads in strength of concrete.

1.4 Limitations of the study

Some of the limitations of the project are as follows.

- Use of *Bacillus Subtilis* only.
- Use of one M30 concrete design mix only.
- Use of Calcium alginate only as shell material.
- Self-Healing Monitoring for 56 days only.
- No RCPT and other non-destructive tests on concrete.

CHAPTER 2: LITERATURE REVIEW

Literature Review was done by assessing various journals and their research articles and review articles. Autogenous self-healing was achieved by a number of ways. Firstly, addition of encapsulated bacteria, secondly, specific type of fungi addition in concrete has been used as biological pathway for self-healing. Similarly, polymer based self-healing such as use of carbonic anhydrase and poly methylmethacrylate (PMMA) has been developed recently (Taheri & Clark, 2021). Bacterial encapsulation is cheaper, easier and easily available alternative among above mentioned alternatives in case of Nepal.

2.1 Previous Studies self-healing concrete with bacterial encapsulation

Virginie Wiktor et al investigated the effects of introducing *Bacillus Sphaericus* encapsulated in modified alginate-based hydrogel and proved excellent self-healing characteristics in cement concrete as well as cement mortar (J. Wang et al., 2015).

Henk M. Jonkers et al engineered bacteria based self-healing cementitious material for usage in low temperature saline water environments. Through compression testing and measurements of the crack water permeability, the composite was evaluated for its ability to repair cracks and generate strength. Following 98 days of immersion in artificial saltwater at 8°C, the composite showed outstanding crack-healing abilities. The cracks were attributed to autonomous precipitation, autonomous bead swelling, magnesium-based mineral precipitation, and bacteria-induced calcium-based mineral precipitation within and on the surface of the bacteria-based beads. However, compared to ordinary mortar specimens, mortar specimens containing beads showed lower compressive strengths. The development of a bacteria activated organic-inorganic composite healing material is an exciting new direction for self-healing concrete research (Palin et al., 2017).

Mostafa Seifan et al. suggested calcium alginate as a shielding carrier to boost bacterial resistance to harsh environmental conditions. The model demonstrated that the maximum concentration of $CaCO_3$ is obtained when the bacteria are inactivated in calcium alginate beads made using 1.38% (w/v) Sodium Alginate and 0.13 M Calcium Chloride. (Seifan et al., 2017).

Renee M. Mors et al. carried out demonstration projects that portrayed the use of bacteria-based self-healing agents on a large scale. These demonstration projects demonstrated the safety of adding the bacteria-based self-healing agent to the concrete mix since no adverse

impacts on building quality were found. However, given that there was scarcely any cracking in the demonstration structures, it was also challenging to uncover evidence for improved crack-healing ability (Mors & Jonkers, 2019).

Saman Shahid et al. used several bacillus strains to encapsulate microorganisms in sodium alginate beads. The compressed strength of the concrete cubes was not compromised by the encapsulated bacterial mix, which made up 2-3% of the entire volume. The use of Bacillus Subtilis led to a 16% improvement in concrete's compressive strength as well as considerable healing. Only a 6% improvement in concrete strength was attained when *Bacillus Anthracis* was used, though. The *Bacillus Pasteurii* also failed to provide any useful findings. Comparatively speaking, *Bacillus Subtilis* produced superior outcomes. For compressive strength and fracture self-healing, bacterial cultures in sodium alginate beads at a concentration of 2% to 3% worked best (Shahid et al., 2020).

Elhem Ghorbel et al. mixed peptone, yeast extract and *Bacillus Subtilis* as microbial adjunct in concrete mix design. They discovered that a decrease in porosity led to an increment in strength and dynamic modulus and a decrease in water absorption, gas permeability, and chloride penetration (Nguyen et al., 2019).

Miaomiao Gao et al. developed a novel hydrogel that was crosslinked by alginate, chitosan, and calcium ions for the purpose of encasing bacteria. The swelling capabilities of calcium alginate were shown to be enhanced by the addition of chitosan (Gao et al., 2020).

Xin Chen et al. suggested that there is a risk that the bacterium capsules or other carriers may break and release the self-healing components as a result of the shearing action in the concrete mixer. The qualities of the concrete might be negatively impacted, although the effectiveness of self-healing would be affected. Instead of focusing on the possible effectiveness of self-healing in a structural service, their investigation examined the impacts of component growth media with various components incorporating germination and sporulation aids for the bacterial aerobic oxidation pathway on the fundamental characteristics of fresh and hardened concrete. Tests were conducted to determine the effects of growth media on air content, fluidity, capillary absorption, strength development of cement mortar in accordance with the relevant standards. According to the research, a multi-constituent growth media won't significantly alter the characteristics of concrete in the amounts that are expected to be released during mixing (Chen et al., 2019).

Palin et al. created calcium alginate beads based on bacteria for marine conditions with low temperatures. In a fluid that simulated a coastal concrete fracture, the beads were examined for oxygen consumption, swelling, and their capacity to create a biocomposite (Palin et al., 2017).

Elzbieta Stanaszek-Tomal investigated the expense of using microbial concrete vs traditional concrete. It is one of the key reasons why this material is not presently being manufactured in large quantities and used in the building sector. The cost investigation showed that the cost of microbiological concrete is 2.3 to 3.9 times more expensive than the cost of regular, lower-quality concrete. The beginning expenses are by an order of magnitude more than for conventional concrete due to the high cost of the bacterial cultures employed in the material's development (bacteria and nutrients cost about 80% of the cost of raw materials) (Stanaszek-Tomal, 2020).

2.2 Research Gaps

Palin et al. worked extensively on bacterial beads for low temperature marine environment. It is the continuation of their research as self-healing property in concrete were not published before. Also, the beads were tested in simulative marine concrete crack solution (SMCCS) but not in fresh water.

Therefore, in this thesis, changes in compressive strength and self-healing properties of the beads are tested in concrete experimentally. Efficacy of self-healing beads upon fresh water immersion as well as ambient environment is studied. Similarly, changes in dissolved oxygen levels of tap water upon immersion of bacterial beads is studied.

CHAPTER 3: MATERIALS AND METHODS

3.1 Materials Required

- Alginic acid sodium salt from brown algae (Sigma Aldrich)
- Magnesium Acetate
- Calcium Acetate
- Yeast Extract
- Cement
- Coarse Aggregate
- Fine Aggregate
- High Range Water Reducing Admixture

3.2 Apparatus Required

- Beaker
- Infusion Set
- Plastic box
- Measuring Cylinder
- Weighing Balance
- Stir rod
- Infusion Set
- Magnetic Stirrer
- FTIR spectroscope
- Stereo microscope
- Energy Dispersive Spectroscope
- Cube moulds
- Concrete Cutter
- Compressive Strength Testing Machine

3.3 Methodology

Before the methodology began, necessary materials were procured and vital logistics had to be planned as well as procured. Methodology of the study can be divided largely into three different processes as shown in the figure below namely Beads Development, Beads

Characterization and Self-healing Characterization. Each step in the process required various techniques and processes.

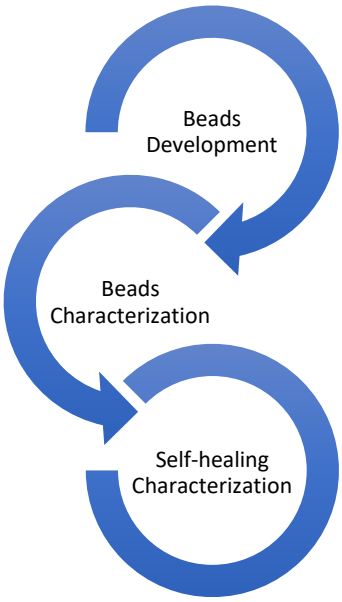

Figure 3:Methodology for development and characterization of self-healing concrete

3.3.1 Beads Development

A nutritional medium containing 5 gl^{-1} of peptone, 5 gl^{-1} of sodium chloride, 1.5 gl^{-1} of beef extract, and 1.5 gl^{-1} of yeast extract was used to cultivate the ATCC bacteria. 1.5% (w/v) sodium alginate (Sigma-Aldrich), 6.4 gl^{-1} of magnesium acetate tetrahydate (SRL), 0.48 gl^{-1} of yeast extract, and 2 mll^{-1} of nutritional medium containing *Bacillus subtilis* were combined to create a precursor solution. Through an IV infusion set and a needle with a diameter of 0.8 mm, the precursor solution was injected dropwise into a calcium acetate gelling solution (6.4 gl1) (SRL) at a height of 17 cm. Upon entering the calcium acetate solution, these droplets cross-polymerized to form calcium alginate beads. The bacteria-filled BCAB beads were created in batches and taken from the calcium acetate solution. They were then washed three times in distilled water and dried for 12 hours on a piece of paper. As a control, bacteria-free beads i.e. CABs (calcium alginate beads containing magnesium acetate and yeast extract) were created. All beads were kept in dry, airtight conditions before to use in experiments. Following the below mentioned reactions, the bacteria in this study have the ability to cause calcium carbonate precipitation.

$$\underset{\text{Organic mineral precursor compound}}{(CH_2O)n} + O_2 \xrightarrow{\text{Bacteria}} CO_2 + H_2O, \quad (1)$$

$$CO_2 + H_2O \leftrightarrow H_2CO_3, \quad (2)$$

$$H_2CO_3 \leftrightarrow HCO_3^- + H^+, \quad (3)$$

$$2HCO_3^- \leftrightarrow CO_3^{2-} + CO_2 + H_2O, \quad (4)$$

$$Ca^{2+} + CO_3^{2-} \leftrightarrow CaCO_3. \quad (5)$$

During the procedure described above, oxygen is used. So, to measure the bacterial activity in beads, DO assays are utilized (Palin et al., 2016).

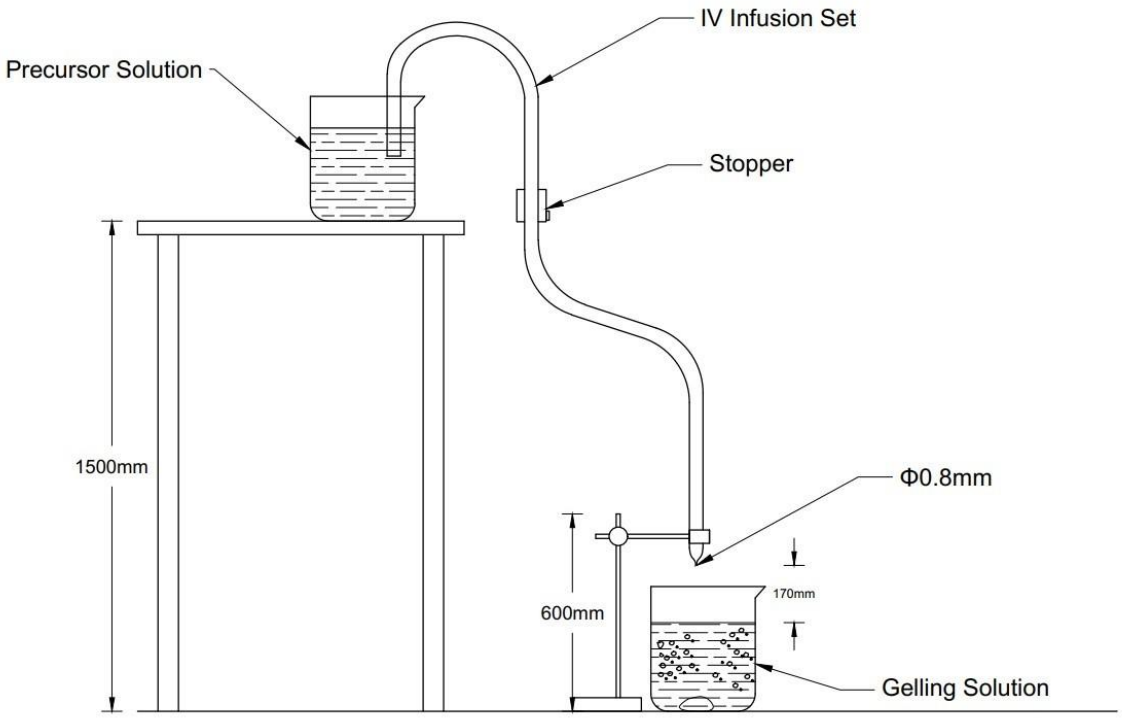

Figure 4: Preparation of BCAB

3.3.2 Beads Characterization

CAB and BCAB were oven dried for 12 hours at 60^{o}C and ground in porcelain basin forming powder which in turn was used for FTIR spectroscopy and was sent for SEM analysis in an air tight pouch. The beads were frozen in refrigerator at -18^{o}C and cut in half using scalpel and was sent for Energy Dispersive Spectroscopy (EDS) in an air tight pouch. Also, the beads were immersed in a 300ml bottle for monitoring DO changes.

3.3.3 Self-healing Characterization

Twelve 150mm M30 grade concrete cubes were cast as control. The concrete cubes were designed by ACI method of mix design. Aggregate and cement properties were tested as per the requirement. Half a dozen of M30 concrete cubes with CAB were cast for each 1.5%, 2% and 2.5% (by volume). A dozen of M30 concrete cubes with BCAB were cast for each 1.5%, 2% and 2.5% (by volume).

Description	Name	Number of concrete cube (150mm) samples	Wet Volume of concrete in m^3	Dry volume of concrete in m^3	Concentration	Volume of beads(m^3)	Volume of beads (ml)	Volume of Calcium alginate beads(ml)
Control M30		12	0.041	0.062				
M30 with CAB	CAB	6	0.020	0.031	1.5% by vol	0.0004617	462	
	CAB1	6	0.020	0.031	2% by vol	0.0006156	616	
	CAB2	6	0.020	0.031	2.5% by vol	0.0007695	770	1846.8
M30 with BCAB	BS	12	0.041	0.062	1.5% by vol	0.0009234	923	
	BS1	12	0.041	0.062	2% by vol	0.0012312	1231	
	BS2	12	0.041	0.062	2.5% by vol	0.0015390	1539	3693.6
Sum		66	0.223	0.339				

Table 1: Concrete Experiment Design

Approximate Solution (ml)	Sodium Alginate (1.5% w/v) (g)	Magnesium Acetate ($6.4l^{-1}$)	Yeast Extract ($0.48\ l^{-1}$)	Calcium Acetate ($6.4\ l^{-1}$)	Bacterial Spores($7*10^8\ l^{-1}$)	Distilled Water(ml)
2000	30	12.8	0.96	12.8	-	1970
5000	75	32	2.4	32	3.5*10^9	4925
Sum	105	44.8	3.36	44.8	3.5*10^9	6895

Table 2: Calculations for beads development

Aggregate properties to be tested for conducting ACI method of mix design were conducted and the results were obtained as following.

Sanga sample had better particle size distribution than Nuwakot sample, therefore, sanga sample was chosen.

Average Fineness modulus of sanga FA was found to be 2.78.

Dry rodded bulk density of CA was found to be 1575.61 kg/m^3.

Water content of CA was found to be nearly equal to 0%.

Water content of FA was found to be 8%.

Bulk specific gravity (SSD) condition of CA was found to be 1636.

ACI Method of mix design was conducted as following.

ACI Method Concrete Mix Design
Concrete of 28 day Characteristics Compressive Strength 30MPa

Step 1: Slump Determination

From table 22

Adopt Placing Condition	Concreting of lightly reinforced sections with vibration
Degree of workability	Medium
Values of workability	25mm-75mm slump for 20mm maximum nominal aggregat

Step 2: Maximum Size of coarse aggregate

Adopt maximum size of coarse aggregate as 20mm

Step 3: Water Cement Ratio determination

30MPa= 305.81kgf/cm^2

From table 31, Interpolating;

We get water cement ratio by weight as 0.541

Step 4: Approximate mixing water for the desired workability and maximum size of coarse aggregate

From table 32

For slump	3cm to 5cm
Maximum Size of aggregate	20mm
For non air entrained concrete	
Adopt approximate mixing water	185 kg/m^3

Step 5: Cement Content Determination and check

Cement Content	Water content / Water cement ratio
	185/0.541
	341.98 kg/m^3

Check based on exposure condition, from table 5

Maximum Size of coarse aggregate	20mm
Type of Concrete	Reinforced concrete
Exposure	Severe
Maximum free water cement ratio	0.45
Minimum Cement Content	320 kg/m^3
Adopt water cement ratio	0.45
Cement Content to be used	185/0.45
	411 kg/m^3

Use of high range water reducing admixture ASTM C-494-1981(Type G)

(0.2%-1.5%of cement weight(w/w)) decreases the water content 12% to 30 %
So, reducing water content by 20 % i.e.

Use mixing water	185*0.8
	148 kg/m^3
Actual Water cement ratio	0.36
Use high range water reducing admixture	0.7% of cement content i.e 2.88 kg/m3

Step 6:Determination of amount of coarse aggregate

Fineness Modulus of Sand	2.78 (Sankhu Sample)
Maximum Size of Coarse Aggregate	20mm

Volume of dry rodded coarse aggregate per unit volume of concrete by table 33
Interpolating we get, for 20mm coarse aggregate and 2.78 fineness modulus

Volume of dry rodded coarse aggregate per unit volume of concrete	0.622
Dry rodded bulk density of the aggrega	1575.61 kg/m^3 (Sankhu Sample)
Dry weight of coarse aggregate	0.622*1575.61
	980.03 kg/m^3

Step 7: Determination of amount of fine aggregate

Nominal maximum size of coarse aggregate	20mm

For no air entrained concrete

First estimate of weight of fresh concre	2345 kg/m^3
Weight of fine aggregate	Weight of fresh concrete- Weight of all other ingredients
	2345-411-148-980-2.88
	803.12 kg/m3
Weight ratio for trial mix assuming	1:1.95:2.38:0.36

CA and FA as saturated surface dry

Step 8: Water Content Adjustment

Water content in FA	9%
Water content in CA	0.00%
Total free surface moisture in FA	72.28
Weight of FA in field condition	875.40
CA absorbs 4% water	39.20
Weight of CA in field condition	940.83
Water in FA that acts as mixing water	33.08
Actual Water to be used as mixing wate	114.92

3.4 Testing and Evaluation

3.4.1 Testing of beads

3.4.1.1 Dissolved Oxygen test

- Sample water and BCAB were placed in two 300 mL glass Biological Oxygen Demand (BOD) stoppered bottles.

- In the same way, 2 mL of the alkali-iodide-azide reagent was added.

- The bottle was carefully stopped to prevent the introduction of air. By repeatedly inverting, the material was agitated. A precipitate or floc cloud that was brownish orange developed. The sample was mixed by repeatedly flipping it upside down after the floc had sunk to the bottom, and then it was allowed to settle again.

- A pipette was used to add 2 mL of concentrated sulfuric acid, which was held immediately above the sample. To remove the floc, it was gently stoppered and turned upside down numerous times. The sample was now "fixed" and could be retained for up to 8 hours in a cold, dark environment. The bottle was sealed with the help of aluminum foil and a rubber band throughout the storage period, and distilled water was squirted along the stopper as an extra precaution.

- 20 mL of the sample was titrated with sodium thiosulfate in a glass flask to a straw-colored hue. The sample water was continuously stirred or swirled as the titrant solution was progressively poured into the flask using a calibrated pipette.

- 2 mL of starch solution was added to ensure blue color formed.

- The sample was slowly titrated until it became clear. When the experiment's goal was accomplished, the blue hue could be removed with just one drop of the titrant. DO was calculated using the formula:

D.O. in **mg/lit = 8×100×N/V×v**

where: V = Volume of sample taken (ml)

v = Volume of used titrant (ml)

N = Normality of titrant

3.4.1.2 FTIR spectroscopy analysis

Fourier Transform Infrared Spectroscopy (FTIR) tests are used to differentiate organic, polymeric, and, in certain situations, inorganic materials. This method uses infrared light to scan test materials and examine chemical characteristics.

Infrared light from the FTIR instrument is used to irradiate the sample. The infrared radiation ranges from wavelength 10,000 cm^{-1} to 100 cm^{-1}, a part of which is absorbed and a part of which passes through. The absorbed radiation is transformed by sample molecules into rotational and/or vibrational energy. The resultant signal is displayed as a spectrum at the detector and ususally ranges from 4000 cm^{-1} to 400 cm^{-1}. Due to the fact that each chemical structure of molecule provides a unique spectral fingerprint, FTIR analysis is a useful technique for identifying of chemicals.

FTIR analysis is performed to identify as well as pick out contamination if any in CAB and BCAB. The FTIR analysis of samples is performed using the Shimadzu FTIR spectroscope. FTIR spectroscopy test results were interpreted using the research article by Nandiyanto et al.(Nandiyanto et al., 2019).

3.4.1.3 SEM Imaging

A scanning electron microscope (SEM) is a high-resolution microscope that creates pictures of a sample's surface using an electron beam. It enables researchers to view features and structures that are too tiny to be seen using an optical microscope. A beam of electrons is emitted by an electron gun at the top of the microscope column to power the SEM. The sample, which is situated on a platform at the base of the column, is then the target of this beam after it has been focussed by a set of magnetic lenses.

When the electron beam strikes the sample, it interacts with the atoms in the material and causes them to emit secondary electrons. These secondary electrons are then collected by a detector and used to create an image of the surface of the sample. The images produced by an SEM are three-dimensional and can reveal details at a much higher resolution than optical microscopy. SEMs can also be used to analyze the composition of a sample by detecting the characteristic X-rays that are emitted when the electron beam interacts with the atoms in the material.

One of the advantages of an SEM is that it can be used to analyze samples in their natural state, without the need for preparation such as slicing or staining. This makes it a valuable tool in fields such as materials science, biology, and geology.

3.4.1.4 EDS analysis

EDS, sometimes referred to as EDX or XEDS, is an analytical technique for the chemical characterisation and elemental analysis of materials. First, a material is activated by an energy source like electron beam of an electron microscope. Then, core-shell electron is released that helps to release part of the energy. The change in energy is consequently released as an X-ray with a unique spectrum depending on its original atom when a higher energy outer-shell electron moves in to take its place. As a result, it is possible to analyze the composition of a sample volume that has been stimulated by an energy source. Peak's location in the spectrum helps in identifying the element, whilst the element's concentration is reflected by signal's strength.

It has already been mentioned that an electron beam has enough energy to release core-shell electrons and generate X-ray emission. For acquiring compositional data down to the atomic level, EDS detector is attached to an electron microscope. When electron probe scans the material, characteristics X-rays are produced and consequently recorded EDS spectra is assigned to a specific location on the sample. The intensity of the signal and purity of the spectrum both affects how good will be the findings. The materials for making the electron column affects the number of false peaks that can be noticed. Thus, cleanliness is important.

3.4.2 Testing of concrete

3.4.2.1 Compressive Strength test

The IS 516-1959 compression strength test was performed. In order to prevent voids, the concrete was properly tempered and poured into the 150mm concrete molds. Molds were removed after 24 hours, and test specimens were then submerged in water to cure. These specimens had an even, smooth top surface. To do this, cement paste was applied evenly throughout the whole surface of the specimen.

These specimens were tested utilizing a compression testing machine 7 or 28 days after curing. The test specimens were subjected to a constant stress of 140 kg/cm2 until they break.

Concrete's compressive strength was calculated by dividing the load at failure by the specimen's cross sectional area.

3.4.2.2 Self-healing monitoring

Y. H. Loo reported that the microcracks initiated in concrete cylinders at 15% to 40% of the cylinder strength.(Loo, 1991) Concrete cubes were subjected to 40% of characteristic compressive strength in order to induce microcracks. Concrete cubes were cut in half by concrete cutter and observed by Olympus SZ51 Stereomicroscope for 56 days after the cracks had been induced. Images were taken in 2X and 4X magnification.

CHAPTER 4: RESULTS AND DISCUSSION

4.1 Results of tests on beads

4.1.1 FTIR Test Results

FTIR test result of CAB is given below.

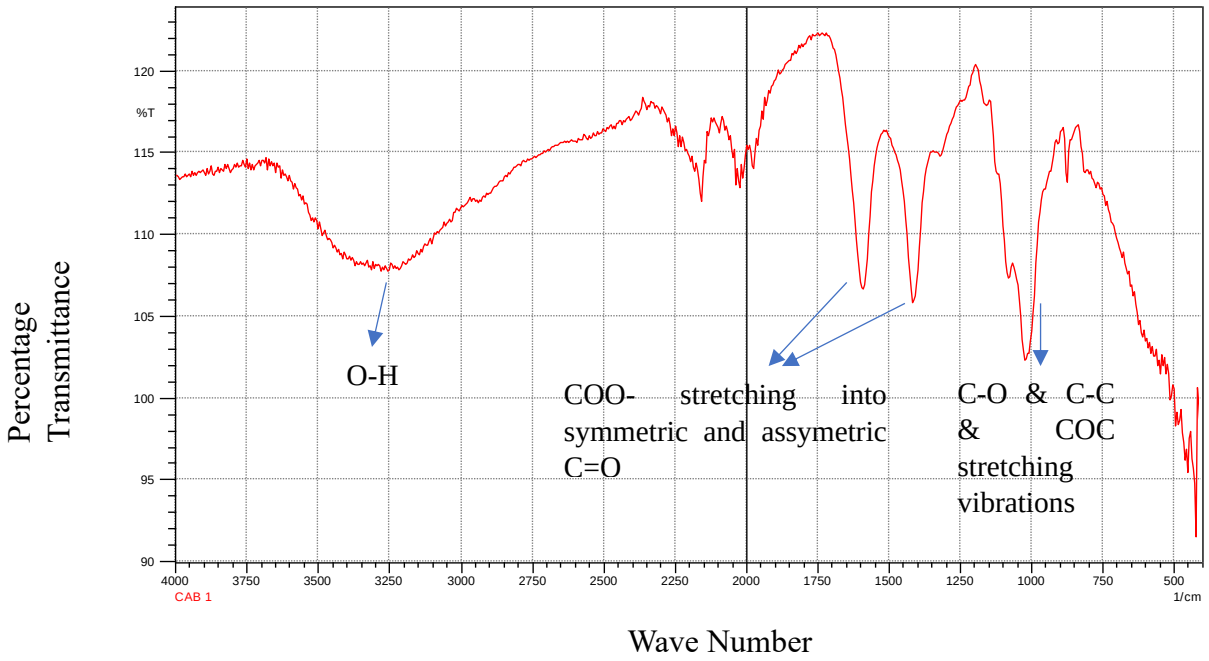

FTIR test result of BCAB is given below.

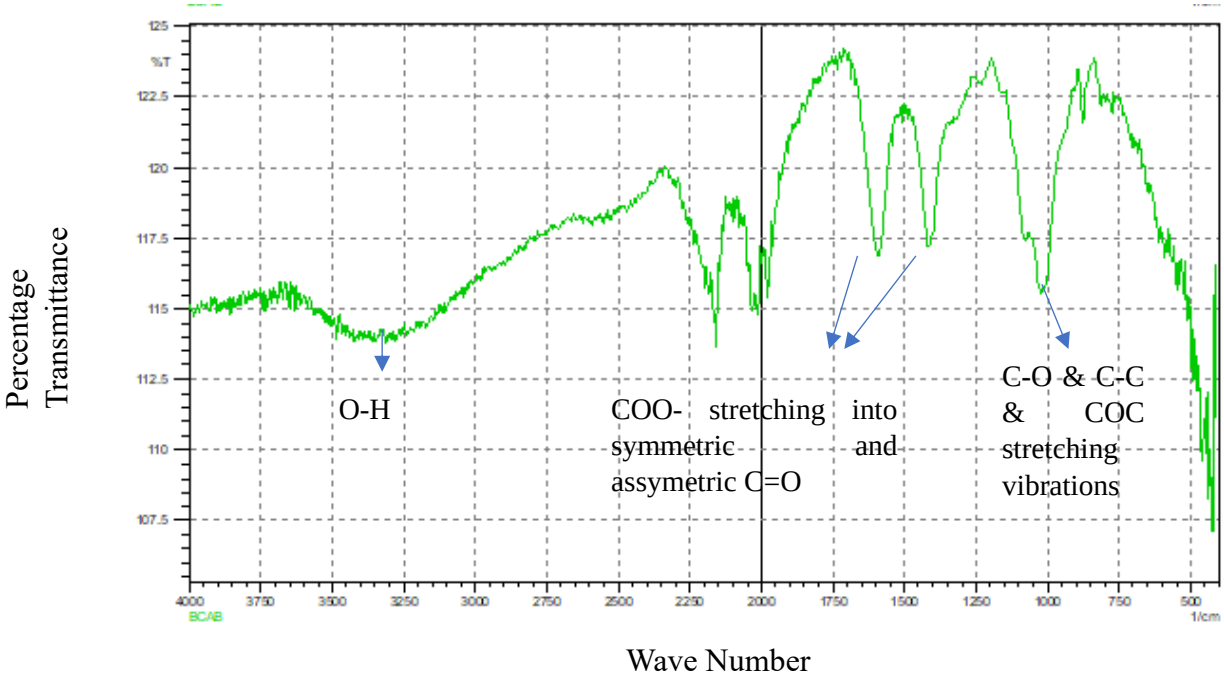

FTIR test result above illustrates various peaks and crevices. We inferred to the research article by Nandiyanto for interpreting the meaning of FTIR test. For FTIR results of CAB and BCAB both, following points could be maintained (Nandiyanto et al., 2019).

1. The peaks contained in single bond area (2500-4000 cm^{-1})

- Broad absorption band was found between 3600 cm^{-1} to 2750 cm^{-1} which represents O-H bonding in the material
- No specific peak for aldehyde has been found between 2700 cm^{-1} and 2800 cm^{-1}.

- Stretching vibrations of aliphatic C-H were observed at 2925 cm^{-1}.

2. The peaks contained in double bond area (1500-2000 cm^{-1}) and fingerprint region (600-1500 cm^{-1}).

- COO- stretching is split into asymmetric and symmetric C=O vibration.
- The first one is found at 1590 cm^{-1} and the second one at 1410 cm^{-1}.
- The bands at 1295 cm^{-1} were attributed to the C-O stretching vibration.

4.1.2 DO Test Results

Day	Volume of sample(ml)	Concurrent volume of titrant (ml)	Normality of titrant	DO in mg/l
1	100	35	1/80	3.50
10	300	nil	1/80	0

Day 10 bacterial beads immersed in water showed no dissolved oxygen content.

4.1.3 EDS Test Results

EDS test result for CAB is given below.

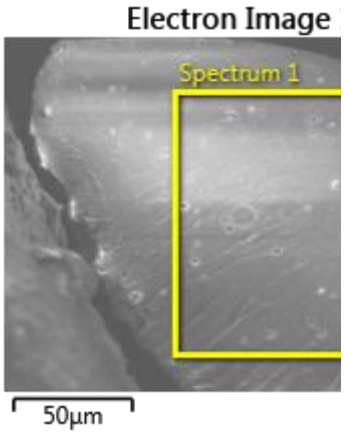

Image 1: Electron Spectrum of CAB

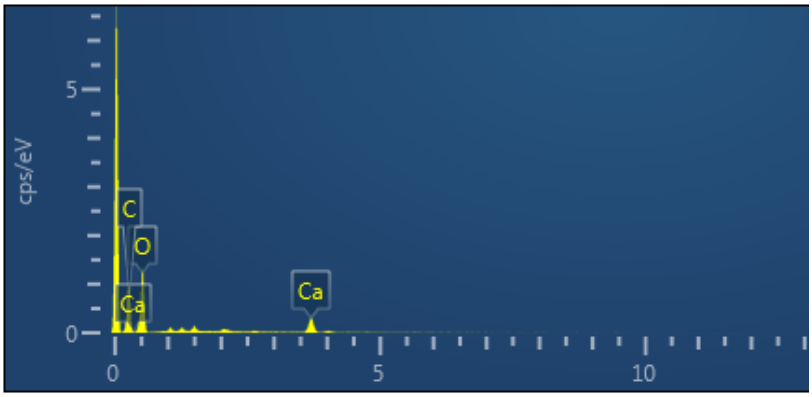

Image 2: Elemental EDS Map of CAB

Element	Line Type	Wt%
C	K series	33.82
O	K series	56.48
Ca	K series	9.70
Total:		100.00

EDS test result for BCAB is given below.

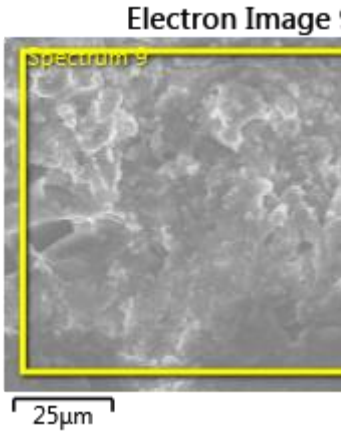

Image 3: Elemental Spectrum of BCAB

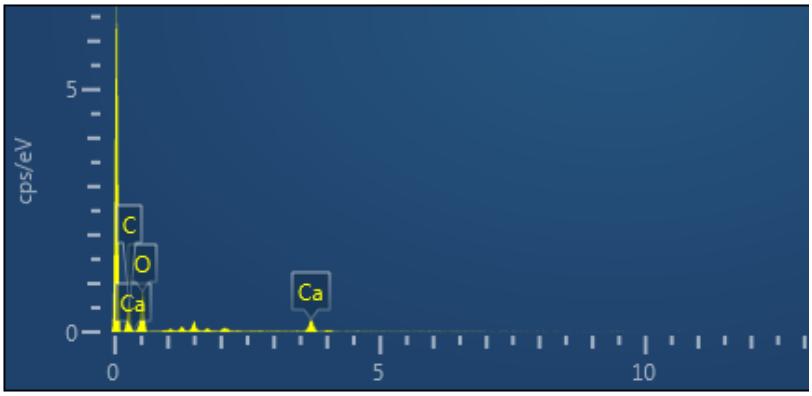

Image 4: Elemental EDS Map of BCAB

Element	Line Type	Wt%
C	K series	30.61
O	K series	57.22
Ca	K series	12.17
Total:		100.00

During the EDX measurement different areas were focused and the corresponding peaks are shown in Figure 5 and 6 for CAB and Figure 7 and 8 for BCAB. In spectrum of CAB, weight percentages of C, O and Ca were 33.82, 56.48, 9.70 respectively. In spectrum of BCAB weight percentages of C, O and Ca were 30.61, 57.22, 12.17 respectively. This confirms the beads were of calcium alginate and higher percentage of Ca in BCAB would be accounted for the formation of calcium carbonate on the surface of BCAB (Ayarza et al., 2017).

4.1.4 SEM images

SEM images of CAB in powder form are given below.

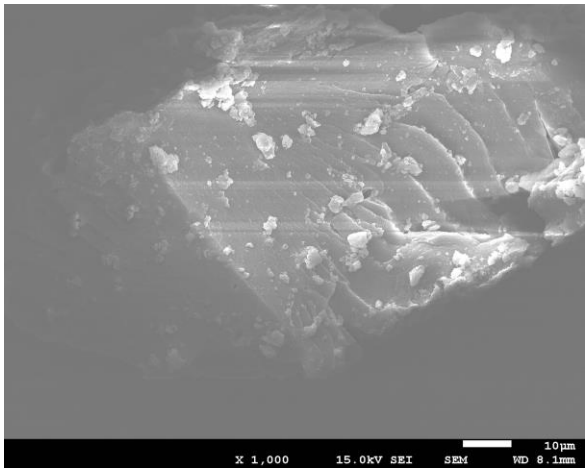

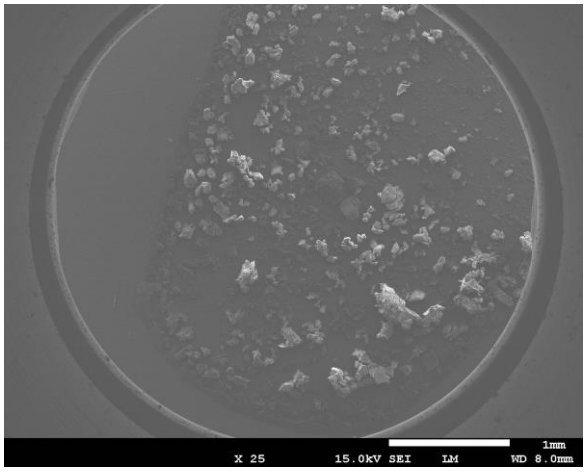

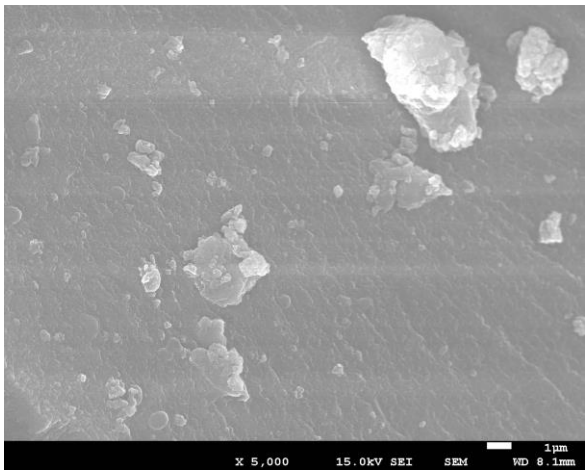

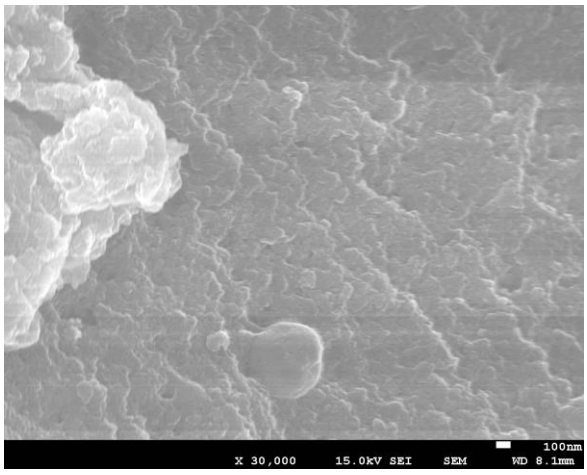

Images 5,6,7,8: SEM images of CAB in different magnifications

SEM images of ground BCAB are given below.

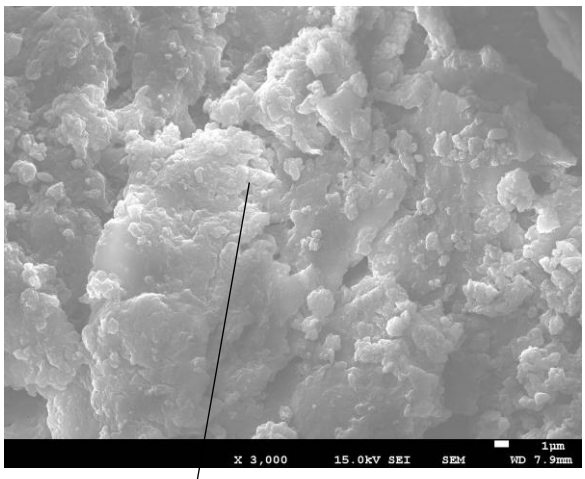

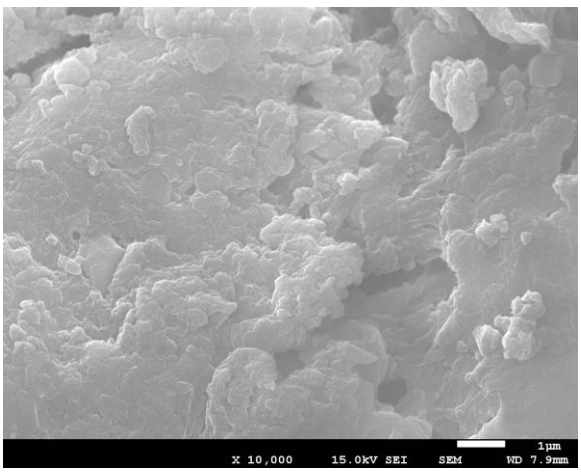

Calcite crystals formation in BCAB

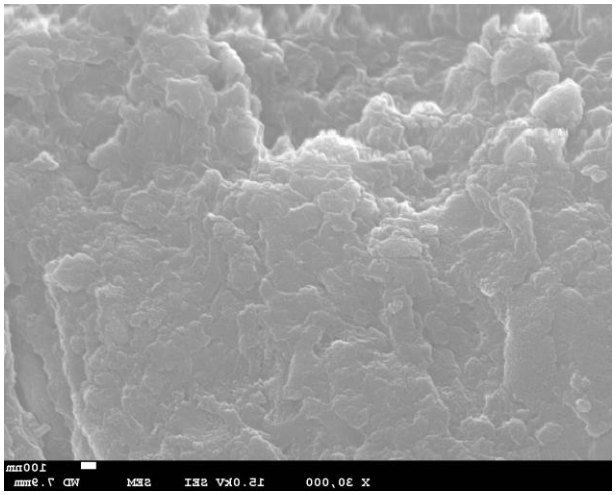

Images 9,10,11: SEM images of BCAB in different magnifications

The images above show porous morphology of CAB and BCAB. BCAB shows some calcite crystal deposition in SEM image analysis.

4.2 Results of tests on concrete

4.2.1 Compressive Strength Test

3 day Compressive Strength Test			
Cube No.	Weight(kg)	Breaking Load(kN)	Compressive Strength(N/mm^2)
1	8.18	374	16.62
2	8.27	314	13.96
3	8.13	342	15.20

7 day Compressive Strength Test			
Cube No.	Weight(kg)	Breaking Load(kN)	Compressive Strength(N/mm^2)
1	8.44	530	23.56
2	8.12	451	20.04
3	8.23	453	20.13

28 day Compressive Strength Test

Cube No.	Weight(kg)	Breaking Load(kN)	Compressive Strength(N/mm^2)
1	8.23	680	30.22
2	8.29	705	31.33
3	8.14	720	32.00
4	8.46	771	34.27
5	8.42	676	30.04
6	8.44	706	31.38

M30 with CAB

For 1.5% concentration(CAB) 7 day compressive strength			
Cube No.	Weight(kg)	Breaking Load(kN)	Compressive Strength(N/mm^2)
1	8.110	568	25.24
2	8.400	540	24.00
3	8.510	554	24.62

For 1.5% concentration(CAB) 28 day compressive strength			
Cube No.	Weight(kg)	Breaking Load(kN)	Compressive Strength(N/mm^2)
1	8.430	726	32.27
2	8.125	754	33.51
3	8.215	760	33.78

For 2% concentration(CAB1) 7 day compressive strength			
Cube No.	Weight(kg)	Breaking Load(kN)	Compressive Strength(N/mm^2)
1	8.185	465	20.67
2	8.280	621	27.60
3	8.100	425	18.89

For 2% concentration(CAB1) 28 day compressive strength			
Cube No.	Weight(kg)	Breaking Load(kN)	Compressive Strength(N/mm^2)
1	8.340	777	34.53
2	8.300	763	33.91
3	8.510	812	36.09

For 2.5% concentration(CAB2) 7 day compressive strength			
Cube No.	Weight(kg)	Breaking Load(kN)	Compressive Strength(N/mm^2)
1	8.205	460	20.44
2	8.215	488	21.69
3	8.310	461	20.49

For 2.5% concentration(CAB2) 28 day compressive strength			
Cube No.	Weight(kg)	Breaking Load(kN)	Compressive Strength(N/mm^2)
1	8.395	704	31.29
2	8.140	667	29.64
3	8.245	652	28.98

M30 with BCAB

For 1.5% concentration(BS) 7 day compressive strength			
Cube No.	Weight(kg)	Breaking Load(kN)	Compressive Strength(N/mm^2)
1	8.430	526	23.38
2	8.125	554	24.62
3	8.215	530	23.56

For 1.5% concentration(BS) 28 day compressive strength			
Cube No.	Weight(kg)	Breaking Load(kN)	Compressive Strength(N/mm^2)
1	8.020	737	32.76
2	8.170	683	30.36
3	8.055	698	31.02

For 2% concentration(BS) 7 day compressive strength			
Cube No.	Weight(kg)	Breaking Load(kN)	Compressive Strength(N/mm^2)
1	8.280	392	17.42
2	8.245	425	18.89
3	8.180	430	19.11

For 2% concentration(BS) 28 day compressive strength			
Cube No.	Weight(kg)	Breaking Load(kN)	Compressive Strength(N/mm^2)
1	8.080	731	32.49
2	8.435	696	30.93
3	8.245	786	34.93

For 2.5% concentration(BS) 7 day compressive strength			
Cube No.	Weight(kg)	Breaking Load(kN)	Compressive Strength(N/mm^2)
1	8.055	402	17.87
2	8.055	475	21.11
3	8.215	304	13.51

For 2.5% concentration(BS) 28 day compressive strength			
Cube No.	Weight(kg)	Breaking Load(kN)	Compressive Strength(N/mm^2)
1	8.115	667	29.64
2	8.270	628	27.91
3	7.990	697	30.98

Above mentioned compressive strength tests are used for analysing the effect of CAB and BCAB in concrete. Turns out they have positive effect in compressive strength of concrete when put in mild concentration.

4.2.2 Self-Healing Monitoring Test Results

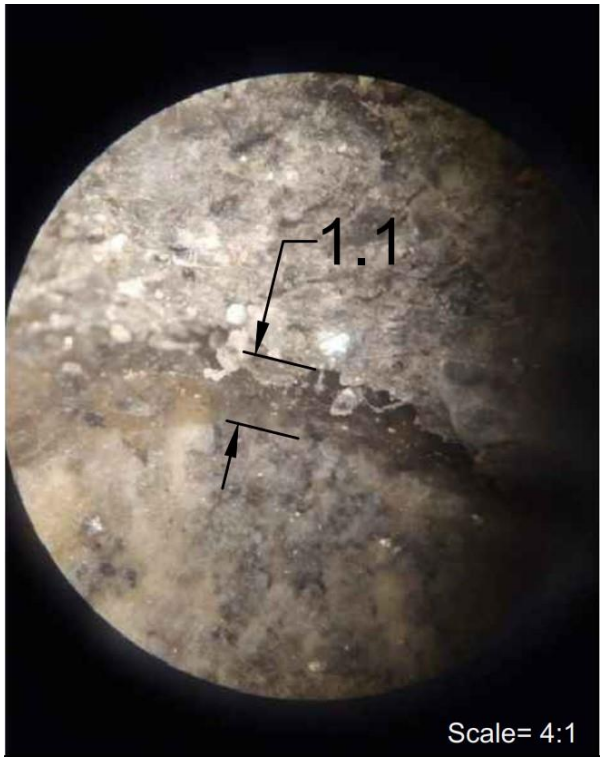

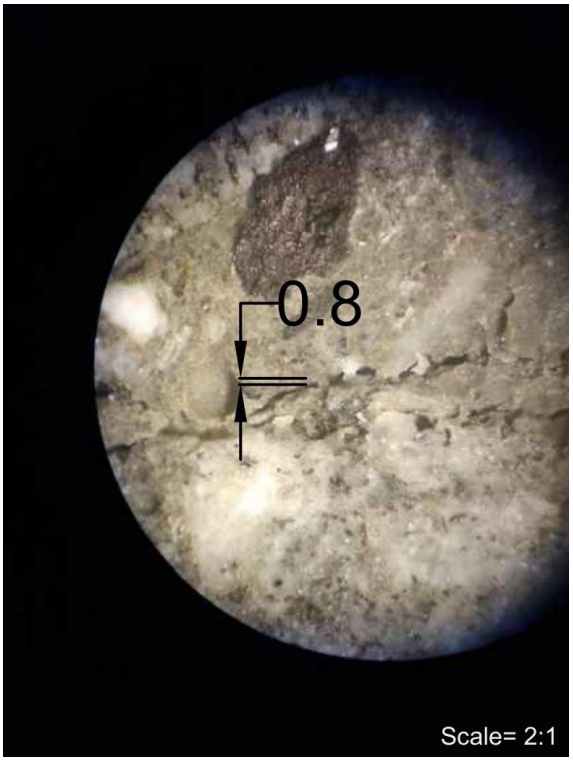

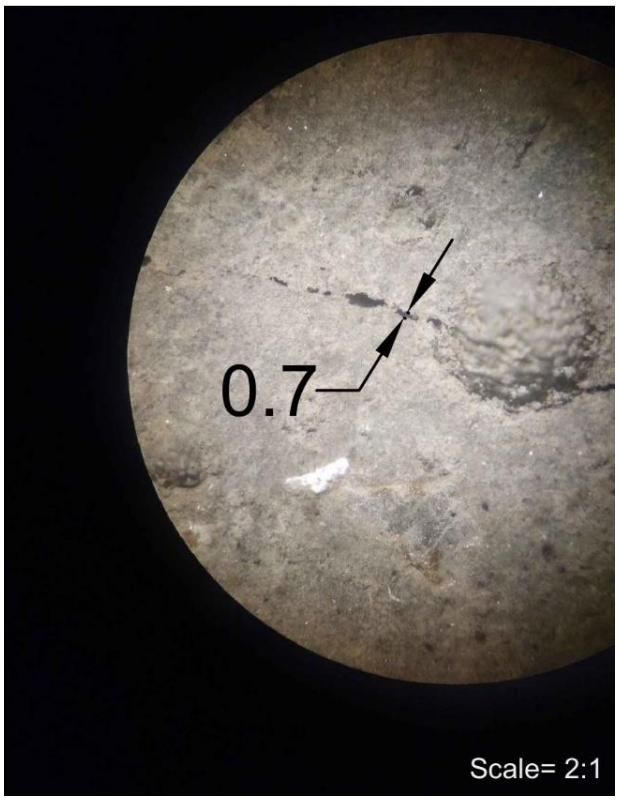

Images 12,13,14,15: Optical images of cracks after 10 days

All units are in mm

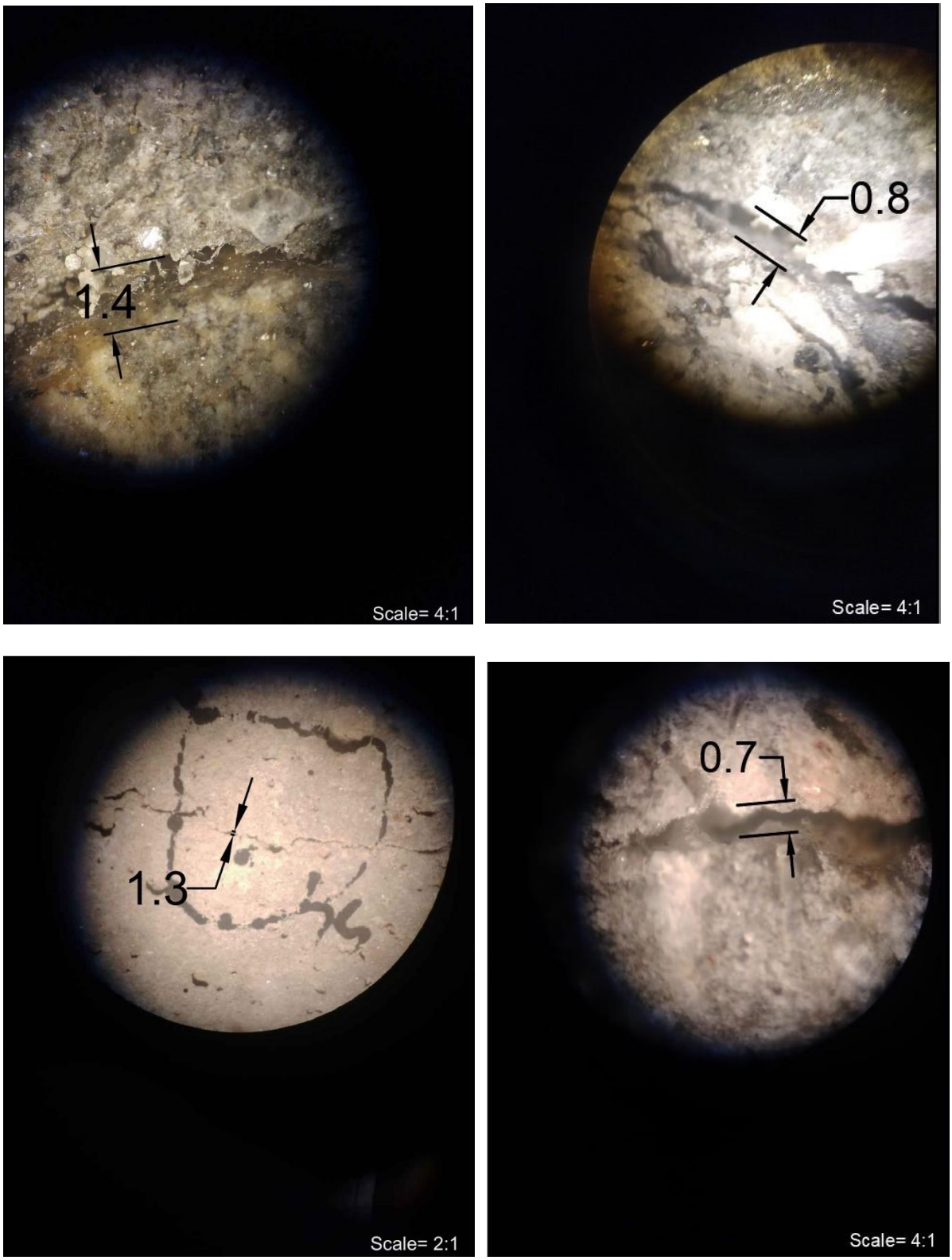

Images 16,17,18,19: Optical images of cracks after 30 days

All units are in mm

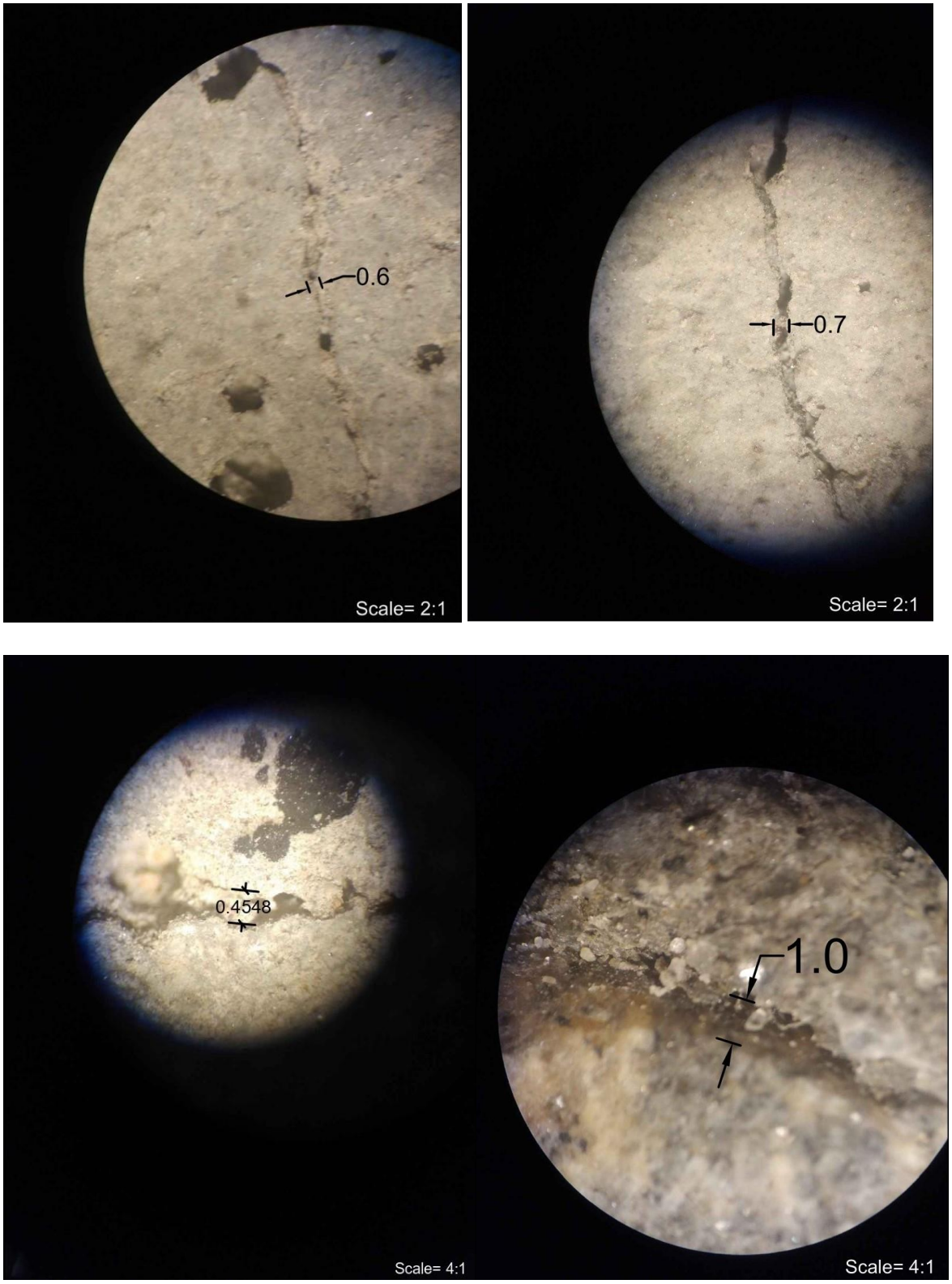

Images 20,21,22,23: Optical images of cracks after 30 days

All units are in mm

4.3 Discussion

4.4 Discussion on tests on beads

4.4.1 Discussion on DO test

DO test result suggests that the bacteria were present in beads after encapsulation as dissolved oxygen was measured to be 0 mg/l after 10 days. It is due to the fact that bacteria consumed dissolved oxygen present in water.

4.4.2 Discussion on FTIR analyses

FTIR analyses proved the presence of O-H bond, COO- bond, C-O bond and C-C bond which are functional groups present in calcium alginate. Consequently, we can identify both CAB and BCAB are made up of calcium alginate.

4.4.3 Discussion on EDS analyses

Atomic weight percentage Results above shows that there is a little increase in Ca weight percentage in BCAB over CAB. Also, C weight percentage has gone down by almost 3% for BCAB over CAB. Elemental EDS map shows no presence of undesired elements i.e. impurities.

Weight percentages of CAB and BCAB indicates the powder were of calcium alginate. Calcium and Carbon concentration increased in BCAB due to the presence of Calcium Carbonate.

4.4.4 Discussion on SEM images

The images are ordered in accordance to their magnification levels. SEM images of CAB illustrates a number of depressions. SEM images of BCAB shows white material in the surface due to the deposition of calcium carbonate or calcite formed by aerobic digestion of bacteria.

4.5 Discussion on tests on concrete

4.5.1 Discussion on compressive strength tests

Concrete cubes with 2% CAB concentration showed maximum average 28-day compressive strength. Also, 2% CAB concentration had maximum 28-day compressive strength.

Similarly, concrete cubes with 2% BCAB had maximum average 28-day compressive strength as well as maximum overall maximum compressive strength.

Concrete cube with CAB showed a little greater compressive strength than control. Also, concrete cubes with BCAB had greater 28-day compressive strength than control cubes by nearly 4 MPa.

4.5.2 Discussion on self-healing characterization

Some images were subjected to 4X magnification i.e., the scale of images is 4:1 while others were subjected to 2X magnification i.e., the scale of images is 2:1. Some cracks were filled partially whereas some cracks were fully filled, whilst other cracks remained as it was. Crack width of 0.7mm were found to be partially or fully healed. Crack width of 1mm and greater were not healed. This may be due to one or more of the following reasons.

- Uneven distribution of BCAB.
- BCAB cracked while hand mixing.
- Low concentration of BCAB.
- Low concentration of Ca^{2+} ions in mixing water and concrete.

CHAPTER 5: CONCLUSION AND RECOMMENDATION

5.1 Conclusion and Recommendations

DO test result implies that the bacteria were present in BCAB. Similarly, EDS and FTIR test results confirmed the formation of calcium alginate beads. Also, tests on concrete cube implied that imparting BCAB in 2% concentration increased compressive strength of concrete by nearly 4 MPa. Self-healing characteristics differed with crack location and crack width. With better distribution mechanism of BCAB and improved method of imparting BCAB, better results could be achieved.

Following could be recommended from the above series of experiments.

- Vascular systems could be used for dispersing the beads. Use of such systems could result in even distribution of beads.
- The beads could produce better results if concrete were submerged in sea water after casting.
- Due to the expensive nature of sodium alginate, research was more costly. Use of clay particles for bacterial encapsulation could be the cheaper alternative.
- A method of detecting the integrity of beads in concrete would be really useful for further projects.
- Analytical techniques such as modelling and simulation could be developed.

REFERENCES

Abramson, S., Meiller, C., Beaunier, P., Dupuis, V., Perrigaud, L., Bée, A., & Cabuil, V. (2010). Highly porous and monodisperse magnetic silica beads prepared by a green templating method. *Journal of Materials Chemistry*, *20*(23), 4916–4924. https://doi.org/10.1039/C000525H

Alcântara, A. C. S., Aranda, P., Darder, M., & Ruiz-Hitzky, E. (2010). Bionanocomposites based on alginate–zein/layered double hydroxide materials as drug delivery systems. *Journal of Materials Chemistry*, *20*(42), 9495–9504. https://doi.org/10.1039/C0JM01211D

Ayarza, J., Coello, Y., & Nakamatsu, J. (2017). SEM–EDS study of ionically cross-linked alginate and alginic acid bead formation. *International Journal of Polymer Analysis and Characterization*, *22*(1), 1–10. https://doi.org/10.1080/1023666X.2016.1219834

Bergdale, T. E., Pinkelman, R. J., Hughes, S. R., Zambelli, B., Ciurli, S., & Bang, S. S. (2012). Engineered biosealant strains producing inorganic and organic biopolymers. *Journal of Biotechnology*, *161*(3), 181–189. https://doi.org/10.1016/J.JBIOTEC.2012.07.001

Chen, X., Yuan, J., & Alazhari, M. (2019). Effect of microbiological growth components for bacteria-based self-healing on the properties of cement mortar. *Materials*, *12*(8). https://doi.org/10.3390/ma12081303

Currey, J. D., & Taylor, J. D. (1974). The mechanical behaviour of some molluscan hard tissues. *Journal of Zoology*, *173*(3), 395–406. https://doi.org/10.1111/J.1469-7998.1974.TB04122.X

Erşan, Y. Ç., Hernandez-Sanabria, E., Boon, N., & de Belie, N. (2016). Enhanced crack closure performance of microbial mortar through nitrate reduction. *Cement and Concrete Composites*, *70*, 159–170. https://doi.org/10.1016/j.cemconcomp.2016.04.001

Gao, M., Guo, J., Cao, H., Wang, H., Xiong, X., Krastev, R., Nie, K., Xu, H., & Liu, L. (2020). Immobilized bacteria with pH-response hydrogel for self-healing of concrete. *Journal of Environmental Management*, *261*. https://doi.org/10.1016/j.jenvman.2020.110225

Hammes, F., & Verstraete, W. (2002). Key roles of pH and calcium metabolism in microbial carbonate precipitation. In *Re/Views in Environmental Science & Bio/Technology* (Vol. 1). http://welcome.to/labmet

Hassoun, M. N., & Al-Manaseer, A. A. (Akthem A.). (n.d.). *Structural concrete : theory and design*. 930. Retrieved February 19, 2023, from https://www.wiley.com/en-sg/Structural+Concrete%3A+Theory+and+Design%2C+7th+Edition-p-9781119605119

Hoffman, A. S. (2012). Hydrogels for biomedical applications. *Advanced Drug Delivery Reviews*, *64*(SUPPL.), 18–23. https://doi.org/10.1016/J.ADDR.2012.09.010

Home | Road Board Nepal. (n.d.). Retrieved February 19, 2023, from https://rbn.org.np/en/

Loo, Y. H. (1991). Some Observations on Microcracking in Concrete under Uniaxial Compression. *Fracture of Engineering Materials and Structures*, 338–347. https://doi.org/10.1007/978-94-011-3650-1_49

Mohammad, I., Khattab, A., Shekha, H., & Abdi, M. A. (2019). *Study on Self-healing Concrete types-A review*. *2*(1), 76–87. https://doi.org/10.26392/SSM.2019.02.01.076

Mors, R. M., & Jonkers, H. M. (2019). Bacteria-based self-healing concrete: Evaluation of full scale demonstrator projects. *RILEM Technical Letters*, *4*, 138–144. https://doi.org/10.21809/rilemtechlett.2019.93

Nandiyanto, A. B. D., Oktiani, R., & Ragadhita, R. (2019). How to read and interpret ftir spectroscope of organic material. *Indonesian Journal of Science and Technology*, *4*(1), 97–118. https://doi.org/10.17509/ijost.v4i1.15806

Neville, A. M. (2011). Properties of concrete-5th edition. *Concrete Mix Design, Quality Control and Specification*, 28–40.

Nguyen, T. H., Ghorbel, E., Fares, H., & Cousture, A. (2019). Bacterial self-healing of concrete and durability assessment. *Cement and Concrete Composites*, *104*. https://doi.org/10.1016/j.cemconcomp.2019.103340

Olderay, M., Xie, M., Strand, B. L., Flaten, E. M., Sikorski, P., & Andreassen, J. P. (2009). Growth and nucleation of calcium carbonate vaterite crystals in presence of alginate. *Crystal Growth and Design*, *9*(12), 5176–5183. https://doi.org/10.1021/CG9005604/ASSET/IMAGES/MEDIUM/CG-2009-005604_0010.GIF

Palin, D., Wiktor, V., & Jonkers, H. M. (2016). A bacteria-based bead for possible self-healing marine concrete applications. *Smart Materials and Structures*, *25*(8). https://doi.org/10.1088/0964-1726/25/8/084008

Palin, D., Wiktor, V., & Jonkers, H. M. (2017). A bacteria-based self-healing cementitious composite for application in low-temperature marine environments. *Biomimetics*, *2*(3). https://doi.org/10.3390/biomimetics2030013

Roy, R., Rossi, E., Silfwerbrand, J., & Jonkers, H. (2020a). Encapsulation Techniques and Test Methods of Evaluating the Bacteria-Based Self-Healing Efficiency of Concrete: A Literature Review. *Nordic Concrete Research*, *62*(1), 63–85. https://doi.org/10.2478/ncr-2020-0006

Roy, R., Rossi, E., Silfwerbrand, J., & Jonkers, H. (2020b). Encapsulation Techniques and Test Methods of Evaluating the Bacteria-Based Self-Healing Efficiency of Concrete: A Literature Review. *Nordic Concrete Research*, *62*(1), 63–85. https://doi.org/10.2478/ncr-2020-0006

Seifan, M., Samani, A. K., Hewitt, S., & Berenjian, A. (2017). The effect of cell immobilization by calcium alginate on bacterially induced calcium carbonate precipitation. *Fermentation*, *3*(4). https://doi.org/10.3390/fermentation3040057

Shahid, S., Aslam, M. A., Ali, S., Zameer, M., & Faisal, M. (2020). Self-Healing of Cracks in Concrete Using Bacillus Strains Encapsulated in Sodium Alginate Beads. *ChemistrySelect*, *5*(1), 312–323. https://doi.org/10.1002/slct.201902206

Stanaszek-Tomal, E. (2020). Bacterial concrete as a sustainable building material? In *Sustainability (Switzerland)* (Vol. 12, Issue 2). MDPI. https://doi.org/10.3390/su12020696

Taheri, S., & Clark, S. M. (2021). Preparation of Self-healing Additives for Concrete via Miniemulsion Polymerization: Formulation and Production Challenges. *International Journal of Concrete Structures and Materials*, *15*(1), 1–15. https://doi.org/10.1186/S40069-020-00449-2/FIGURES/9

van Tittelboom, K., & de Belie, N. (2013). Self-healing in cementitious materials-a review. *Materials*, *6*(6), 2182–2217. https://doi.org/10.3390/MA6062182

van Tittelboom, K., de Belie, N., de Muynck, W., & Verstraete, W. (2010). Use of bacteria to repair cracks in concrete. *Cement and Concrete Research*, *40*(1), 157–166. https://doi.org/10.1016/j.cemconres.2009.08.025

Wang, J., Mignon, A., Snoeck, D., Wiktor, V., van Vliergerghe, S., Boon, N., & de Belie, N. (2015a). Application of modified-alginate encapsulated carbonate producing bacteria in concrete: a promising strategy for crack self-healing. *Frontiers in Microbiology*, *6*(OCT). https://doi.org/10.3389/FMICB.2015.01088

Wang, J., Mignon, A., Snoeck, D., Wiktor, V., van Vliergerghe, S., Boon, N., & de Belie, N. (2015b). Application of modified-alginate encapsulated carbonate producing bacteria in concrete: A promising strategy for crack self-healing. *Frontiers in Microbiology*, *6*(OCT). https://doi.org/10.3389/fmicb.2015.01088

Wang, J. Y., Soens, H., Verstraete, W., & de Belie, N. (2014). Self-healing concrete by use of microencapsulated bacterial spores. *Cement and Concrete Research*, *56*, 139–152. https://doi.org/10.1016/J.CEMCONRES.2013.11.009

Wegst, U. G. K., & Ashby, M. F. (2004). The mechanical efficiency of natural materials. *Philosophical Magazine*, *84*(21), 2167–2186. https://doi.org/10.1080/14786430410001680935

Wiktor, V., & Jonkers, H. M. (2011). Quantification of crack-healing in novel bacteria-based self-healing concrete. *Cement and Concrete Composites*, *33*(7), 763–770. https://doi.org/10.1016/J.CEMCONCOMP.2011.03.012

Wu, J. L., Wang, C. Q., Zhuo, R. X., & Cheng, S. X. (2014). Multi-drug delivery system based on alginate/calcium carbonate hybrid nanoparticles for combination chemotherapy. *Colloids and Surfaces. B, Biointerfaces*, *123*, 498–505. https://doi.org/10.1016/J.COLSURFB.2014.09.047

APPENDIX A: Aggregate properties tests data

Determination of fineness modulus of aggregate was done according to ASTM C128 and ASTM C33
Sampling of fine aggregate and coarse aggregate was done according to ASTM D75
Determination of dry rodded bulk density of coarse aggregate was done according to ASTM C29
Seive analysis of coarse aggregate was done according to ASTM C136-01
Specific Gravity of CA was done according to ASTM C 127-88
Specific Gravity of FA was done according to ASTM C 128-97
Water Content of FA and CA was done according to ASTM D2216 − 19

1. Determination of fineness modulus of fine aggregate

Nuwakot sample A
Weight of sample 600g

Seive Size	Weight of seive(g)	Weight of seive and FA(g)	Weight of FA retained (g)	Percentage weight retained (%)	Cumulative percentage weight retained (%)
4.75mm	420	477.5	57.5	9.6	9.6
2.36mm	323	350.5	27.5	4.6	14.2
1.18mm	308.5	385.5	77	12.8	27.0
600µm	344.5	421.5	77	12.8	39.8
300µm	325.5	504.5	179	29.8	69.7
150µm	298.5	429.5	131	21.8	91.5
Pan	400.5	451.5	51	8.5	
			600		251.8
				FM	**2.52**

Nuwakot Sample B
Weight of sample 600g

Seive Size	Weight of seive(g)	Weight of seive and FA(g)	Weight of FA retained (g)	Percentage weight retained (%)	Cumulative percentage weight retained (%)
4.75mm	420	499.5	79.5	13.3	13.3
2.36mm	323	355.5	32.5	5.4	18.7
1.18mm	308.5	387.5	79	13.2	31.8
600µm	344.5	420.5	76	12.7	44.5
300µm	325.5	497.5	172	28.7	73.2
150µm	298.5	416.5	118	19.7	92.8
Pan	400.5	443.5	43	7.2	
			600		274.3
				FM	**2.74**

Nuwakot Sample C
Weight of sample 600g

Seive Size	Weight of seive(g)	Weight of seive and FA(g)	Weight of FA retained (g)	Percentage weight retained (%)	Cumulative percentage weight retained (%)
4.75mm	420	504.5	84.5	14.1	14.1
2.36mm	323	351.5	28.5	4.8	18.8
1.18mm	308.5	392	83.5	13.9	32.8
600µm	344.5	419.5	75	12.5	45.3
300µm	325.5	494	168.5	28.1	73.3
150µm	298.5	414.5	116	19.3	92.7
Pan	400.5	444.5	44	7.3	
			600		276.9
				FM	**2.77**

Average fineness modulus of FA of Nuwakot sample	**2.68**

Sankhu Sample A
Weight of sample 600g

Seive Size	Weight of seive(g)	Weight of seive and FA(g)	Weight of FA retained (g)	Percentage weight retained	Cumulative percentage weight
4.75mm	420	502.5	82.5	13.8	13.8
2.36mm	323	345	24.5	4.1	17.8
1.18mm	308.5	416.5	108	18.0	35.8
600µm	344.5	440.5	96	16.0	51.8
300µm	325.5	455	129.5	21.6	73.4
150µm	298.5	402	103.5	17.3	90.7
Pan	400.5	456.5	56	9.3	
			600		283.3
				FM	**2.83**

Sankhu Sample B
Weight of sample 600g

Seive Size	Weight of seive(g)	Weight of seive and FA(g)	Weight of FA retained (g)	Percentage weight retained	Cumulative percentage weight
4.75mm	420	495	75	12.5	12.5
2.36mm	323	344	21	3.5	16.0
1.18mm	308.5	409.5	101	16.8	32.8
600µm	344.5	442	97.5	16.3	49.1
300µm	325.5	460.5	135	22.5	71.6
150µm	298.5	411	112.5	18.8	90.3
Pan	400.5	458.5	58	9.7	
			600		272.3
				FM	**2.72**

Sankhu Sample C
Weight of sample 600g

Seive Size	Weight of seive(g)	Weight of seive and FA(g)	Weight of FA retained (g)	Percentage weight retained	Cumulative percentage weight
4.75mm	420	501	81	13.5	13.5
2.36mm	323	347	24	4.0	17.5
1.18mm	308.5	410	101.5	16.9	34.4
600µm	344.5	440.5	96	16.0	50.4
300µm	325.5	458	132.5	22.1	72.5
150µm	298.5	410.5	112	18.7	91.2
Pan	400.5	453.5	53	8.8	
			600		279.5
				FM	**2.80**

Average Fineness Modulus of FA of Sankhu Sample	**2.78**

Based on above particle size distribution and Fineness Modulus;
Sankhu sample was found to be better than Nuwakot sample.
Therefore, Nuwakot sample was discarded.

2. Determination of dry rodded bulk density of coarse aggregate

Weight of container 967 g
Weight of water and container 2830 g
Temperature of water 25^0C

Temperature of water(^{0}C)	**Density of water(kgm^{-3})**
21.1	997.97
26.7	996.59
25	?

Interpolating for 25^0C we get density of water as 997.01 kgm^{-3}

Weight of water 1863 g
Volume of water 0.0019 m^3

Sample	Weight of aggregate and container(kg)	Weight of container(kg)	Volume of water(m^3)	Dry rodded Bulk Density(kgm^{-3})
A	3.904	0.967	0.0019	1545.79
B	3.984	0.967	0.0019	1587.89
C	3.994	0.967	0.0019	1593.16
			Mean	1575.61

Hence, dry rodded bulk density was found to be 1575.61 kgm^{-3}

3. Coarse aggregate Seive Analysis

Sample A Sankhu

Seive Size	Weight of seive(g)	Weight of seive and CA(g)	Weight of CA retained (g)	Percentage weight retained	Percentage Passing (%)
19 mm	907.5	1017.5	110	4.4	95.6
12.5 mm	772	2560.5	1788.5	71.54	24.06
9.5 mm	809	1172.5	363.5	14.54	9.52
4.75 mm	812	1023	211	8.44	1.08
Pan	887.5	914.5	27	1.08	0
			2500		

Sample B Sankhu

Seive Size	Weight of seive(g)	Weight of seive and CA(g)	Weight of CA retained (g)	Percentage weight retained	Percentage Passing (%)
19 mm	907.5	1040.5	133	5.32	94.68
12.5 mm	772	2635	1863	74.52	20.16
9.5 mm	809	1112	303	12.12	8.04
4.75 mm	812	996	184	7.36	0.68
Pan	887.5	904.5	17	0.68	0
			2500		

4. Specific Gravity and Water Content of CA and FA

Mass of container A	700 g
Mass of Container B (1010)	853 g
Mass of container C (1051)	838.5 g
Mass of container D (1004)	837.5 g
Mass of container 1051	10.51 g
Mass of container 1004	10.08 g
Mass of container 1010	9.18 g
Mass of container F	874 g
Mass of container B (1010) and field condition CA	1103 g
Mass of container C (1051) and field condition CA	1088.5 g
Mass of container D (1004) and field condition CA	1087.5 g
Mass of container 1051 and field condition FA	30.51 g
Mass of container 1004 and field condition FA	30.08 g
Mass of container 1010 and field condition FA	29.18 g
Mass of container F and field condition FA	3874 g
Mass of container A and field condition of CA	11200 g
Mass of Container B (1010) and oven dry CA	1102.5 g
Mass of container C (1051) and oven dry CA	1087.5 g
Mass of container D (1004) and oven dry CA	1087 g
Mass of container 1051 and oven dry FA	29.16 g

Mass of container 1004 and oven dry FA	28.54 g
Mass of container 1010 and oven dry FA	27.66 g

Sample	Water content	Average values
Container B CA	0.002	
Container C CA	0.004	
Container D CA	0.002	0.003
Container 1051 FA	0.072	
Container 1004 FA	0.083	
Container 1010 FA	0.082	8%

5. Determination of Specific Gravity of CA

Mass of container A and field condition of CA	11200 g
Mass of container A and oven dry CA	10487.5 g
Mass of oven dry CA	9787.5

Dividing above sample into three equal parts i.e. 3262g for CA

The divided sample is immersed in water for 24 hours and weighed.

Sample	Mass of SSD CA in air(g)	Mass of Saturated CA in water(g)	Bulk Specific Gravity (SSD)
Container E	3272	3270	1636
Container C	3272	3270	1636
Container E	3272	3270	1636

Mean bulk specific gravity(SSD) was found to be 1636

APPENDIX B: Cement Test Data

Compressive Strength Test

		3 days result			7 days result			28 days result		
Sample No.		1	2	3	1	2	3	1	2	3
Date of Casting		9/4/2079								
Date of Testing		9/7/2079			9/11/2079			10/2/2079		
Age	days	3			7			28		
Sample Size	mm	70*70*70			70*70*70			70*70*70		
Area of sample	mm^2	4900	4900	4900	4900	4900	4900	4900	4900	4900
Volume of sample	cm^3	343	343	343	343	343	343	343	343	343
Load	kN	181.59	157.17	176.28	221	202.52	213.41	274.52	276.75	284.17
Comp. Strength	N/mm^2	37.058	32.076	35.976	45.102	41.331	43.552	56.025	56.479	57.995
Avg. Comp. Strength	N/mm^2	35.04			43.33			56.83		
Weight	g	845	839	848	854	835	846	845	854	847
Density	T/m^3	2.46	2.45	2.47	2.49	2.43	2.47	2.46	2.49	2.47

APPENDIX C: Tables for ACI method of concrete mix design

TABLE 22 SUGGESTED RANGES OF VALUES OF WORKABILITY OF CONCRETE FOR DIFFERENT PLACING CONDITIONS

(*Clause* 3.1.2.2)

PLACING CONDITIONS	DEGREE OF WORKABILITY	VALUES OF WORKABILITY
(1)	(2)	(3)
Concreting of shallow sections with vibration	Very low	20-10 seconds, Vee-Bee time or 0.75-0.80, compacting factor
Concreting of lightly reinforced sections with vibration	Low	10-5 seconds, Vee-Bee time or 0.80-0.85, compacting factor
Concreting of lightly reinforced sections without vibration, or heavily reinforced sections with vibration	Medium	5-2 seconds, Vee-Bee time or 0.85-0.92, compacting factor or 25-75 mm, slump for 20 mm* aggregate
Concreting of heavily reinforced sections without vibration	High	Above 0.92, compacting factor or 75-125 mm, slump for 20 mm* aggregate

*For smaller aggregate the values will be lower.

TABLE 31 RELATIONSHIP BETWEEN WATER-CEMENT RATIO AND COMPRESSIVE STRENGTH OF CONCRETE

(*Clause* 6.1)

COMPRESSIVE STRENGTH AT 28 DAYS, kgf/cm²	WATER-CEMENT RATIO, BY WEIGHT	
	Non-Air-Entrained Concrete	Air-Entrained Concrete
(1)	(2)	(3)
450	0.38	—
400	0.43	—
350	0.48	0.40
300	0.55	0.46
250	0.62	0.53
200	0.70	0.61
150	0.80	0.71

NOTE — Table 31 is from 'Recommended Practice for Selecting Proportions for Norm·l Weight Concrete' Reported by ACI Committee 211 (ACI Manual of Concrete Practice, Part I, 1979). American Concrete Institute, USA.

TABLE 32 APPROXIMATE MIXING WATER (kg/m^3 OF CONCRETE) REQUIREMENTS FOR DIFFERENT SLUMPS AND MAXIMUM SIZES OF AGGREGATES

(*Clause* 6.1)

SLUMP, cm	MAXIMUM SIZES OF AGGREGATES IN mm							
	10	12.5	20	25	40	50	70	150
	Non-Air-Entrained Concrete							
3 to 5	205	200	185	180	160	155	145	125
8 to 10	225	215	200	195	175	170	160	140
15 to 18	240	230	210	205	185	180	170	—
Approximate amount of entrained air in non-air-entrained concrete, percent	3.0	2.5	2.0	1.5	1.0	0.5	0.3	0.2
	Air-Entrained Concrete							
3 to 5	180	175	165	160	145	140	135	120
8 to 10	200	190	180	175	160	155	150	135
15 to 18	215	205	190	185	170	165	160	—
Recommended average total air content, percent	8.0	7.0	6.0	5.0	4.5	4.0	3.5	3.0

NOTE — Table 32 is from 'Recommended Practice for Selecting Proportions for Normal Weight Concrete' Reported by ACI Committee 211 (ACI Manual of Concrete Practice, Part I, 1979). American Concrete Institute, USA.

Table 5 Minimum Cement Content, Maximum Water-Cement Ratio and Minimum Grade of Concrete for Different Exposures with Normal Weight Aggregates of 20 mm Nominal Maximum Size

(Clauses 6.1.2, 8.2.4.1 *and* 9.1.2*)*

Sl No.	Exposure	Plain Concrete			Reinforced Concrete		
		Minimum Cement Content kg/m³	Maximum Free Water-Cement Ratio	Minimum Grade of Concrete	Minimum Cement Content kg/m³	Maximum Free Water-Cement Ratio	Minimum Grade of Concrete
1)	(2)	(3)	(4)	(5)	(6)	(7)	(8)
i)	Mild	220	0.60	–	300	0.55	M 20
iii)	Moderate	240	0.60	M 15	300	0.50	M 25
iii)	Severe	250	0.50	M 20	320	0.45	M 30
iv)	Very severe	260	0.45	M 20	340	0.45	M 35
v)	Extreme	280	0.40	M 25	360	0.40	M 40

NOTES

1 Cement content prescribed in this table is irrespective of the grades of cement and it is inclusive of additions mentioned in **5.2**. The additions such as fly ash or ground granulated blast furnace slag may be taken into account in the concrete composition with respect to the cement content and water-cement ratio if the suitability is established and as long as the maximum amounts taken into account do not exceed the limit of pozzolona and slag specified in IS 1489 (Part 1) and IS 455 respectively.

2 Minimum grade for plain concrete under mild exposure condition is not specified.

TABLE 33 VOLUME OF DRY-RODDED COARSE AGGREGATE PER UNIT VOLUME OF CONCRETE

(Clause 6.1*)*

Maximum Size of Aggregate mm	Fineness Modulus of Sand			
	2.40	2.60	2.80	3.00
(1)	(2)	(3)	(4)	(5)
10	0.50	0.48	0.46	0.44
12.5	0.59	0.57	0.55	0.53
20	0.66	0.64	0.62	0.60
25	0.71	0.69	0.67	0.65
40	0.76	0.74	0.72	0.70
50	0.78	0.76	0.74	0.72
70	0.81	0.79	0.77	0.75
150	0.87	0.85	0.83	0.81

NOTE — Table 33 is from 'Recommended Practice for Selecting Proportions for Normal Weight Concrete' Reported by ACI Committee 211 (ACI Manual of Concrete Practice, Part I, 1979). American Concrete Institute, USA.

Table 8 First estimate of weight of fresh concrete

First estimate of weight of fresh concrete		
Nominal Maximum size of coarse aggregate (mm)	First estimate of concrete unit weight (kg/m^3)	
	No air entrained concrete	Air – entrained concrete
9.5	2280	2200
12.5	2310	2230
20	2345	2275
25	2380	2290
37.5	2410	2350
50	2445	2345
75	2490	2405
150	2530	2435

APPENDIX D: Images of different processes

Image 24: Precursor Solution preparation on magnetic stirrer

Image 15: Preparation of BCAB

Image 26: Beads in gelling solution

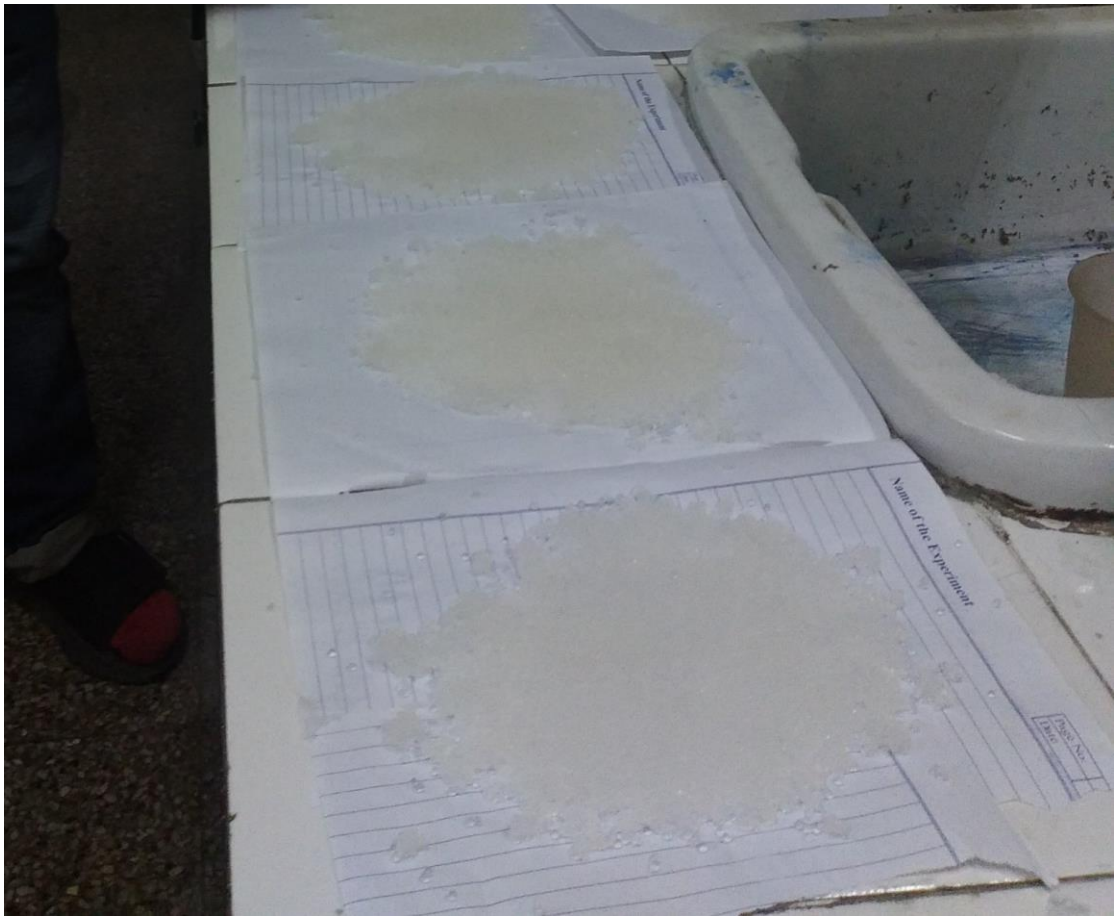

Image 27: BCAB dried in ambient environment

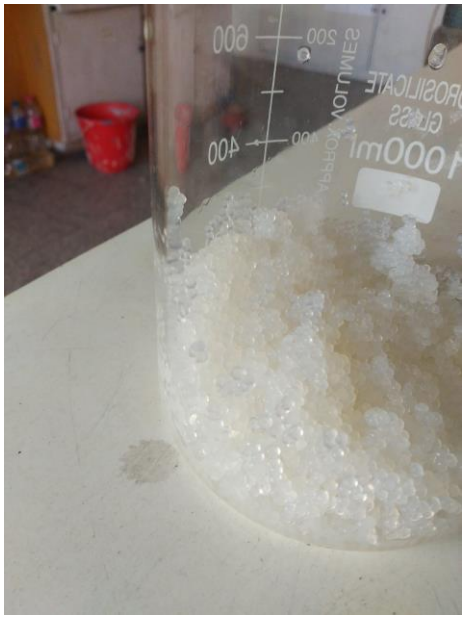

Image 28: BCAB

Image 29: Oven dried BCAB

Image 30: Using Stereomicroscope

Image 31: Concrete Mixing

Image 32: Cube molds preparation